

On the Mechanism of Radical C–N Coupling in Type B Semiconductor Photocatalysis: A High-Pressure Study^{†,§}

Arne Reinheimer, Rudi van Eldik, and Horst Kisch*

Institut für Anorganische Chemie der Universität Erlangen-Nürnberg, Egerlandstr. 1, D-91058 Erlangen, Germany

Received: July 30, 1999

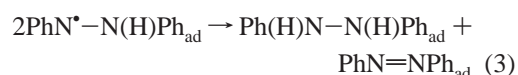
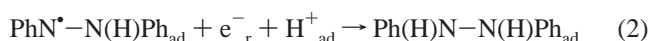
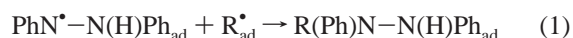
The CdS and CdS/SiO₂ photocatalyzed addition of 2,5-dihydrofuran (2,5-DHF) to azobenzene in methanol solution affords 3-(2,3-dihydrofuryl)hydrazobenzene (**1**) as the major and hydrazobenzene (**2**) as the side product. According to ¹³C NMR and adsorption data, 2,5-DHF is adsorbed parallel to the surface through hydrogen bonding with [OH/SH] groups; adsorption constants of 18 and 30 L mol⁻¹ are obtained for CdS and CdS/SiO₂, respectively. This enhanced effect of the silica support favors formation of the addition product **1**. Different from that, azobenzene exhibits adsorption constants identical within experimental error (11126 and 1059 L mol⁻¹) for both photocatalysts and adsorbs most likely at Brønsted acid centers. These results are corroborated by corresponding adsorption studies with SiO₂. The much better adsorption of 2,5-DHF onto CdS when performed in aqueous suspension is rationalized by comparison of adsorbent and adsorptive polarities, as determined by Reichardt's dye. The absence of any addition products of methanol to a mutual dihydrofuryl radical cation suggests that oxidation by the reactive valence band hole occurs via dissociative electron transfer affording a proton and the dihydrofuryl radical. The latter undergoes C–N coupling with PhN–N(H)Ph, formed in a proton-coupled reduction by the reactive electron, to afford **1**. Formations of **1** and **2** exhibit the same Arrhenius activation energies of 11 kJ mol⁻¹. The rates of both reactions are decreased upon increasing the solvent viscosity by increasing pressure or by using various alcohols. From the average activation volume of 17 cm³mol⁻¹, obtained for **1** and **2** at pressures up to 120 MPa, it is postulated that radical diffusion in the solvent–solute surface multilayer rather than C–N bond formation is the rate-determining step.

Introduction

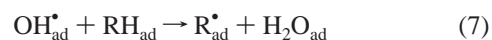
The CdS catalyzed photoaddition of cyclic unsaturated ethers or olefins to 1,2-diazene allows the preparation of hitherto unknown trisubstituted allylhydrazines.¹ It can be classified as type B semiconductor photocatalysis² proceeding via “paired photoelectrolysis”. A typical example is the addition of 2,5-dihydrofuran (2,5-DHF) to azobenzene (Scheme 1). In the proposed mechanism, light absorption by the CdS powder generates electron–hole pairs, which may return to the ground state by radiative and nonradiative recombination or are trapped in emissive and reactive surface sites. The reactive e⁻_r/h⁺_r pair undergoes interfacial electron transfer with adsorbed substrates or nonradiative recombination. Radiative recombination of the charge carriers plays only a minor role, since no emission was detected from the powders employed.³

In the reductive part of the overall reaction, azobenzene is reduced to the PhNH–NPh radical in a proton-coupled reduction. This primary product couples with the oxidatively formed 2,5-dihydrofuryl radical R[•] to give the allyl hydrazine **1** (eq 1). Alternatively, the PhNH–NPh radical is reduced to hydrazobenzene (**2**) by a second proton-coupled reduction (eq 2) or a disproportionation (eq 3). The involvement of intermediary PhNH–NPh and allyl radicals is supported by the appearance of corresponding dimers when the 1,2-diazene is replaced by a

Schiff base.^{2a}



However, three basic mechanistic questions remained unanswered. First, it was unknown how the substrates were adsorbed at the CdS surface. Second, no decision could be made as to whether the radical formation occurs “directly” via a dissociative electron transfer step or through a radical cation followed by fast deprotonation, although thermodynamic estimations favored the former.² Obvious alternatives are two “indirect” routes via intermediate sulfur or OH radicals (eqs 4–7).



Formation of the latter may occur at traces of surface CdO as postulated recently for the photooxidation of ethanol.⁴ And third, it was unclear whether the radical C–N coupling (eq 1) occurred between adsorbed or fully solvated radicals. In the following, we try to answer the first question by investigation of substrate

* Corresponding author. Fax: +9131/8527363. E-mail: Kisch@chemie.uni-erlangen.de.

[†] Heterogeneous Photocatalysis XXII—Part XXI: Reinheimer, A.; Hernández, A.; Kisch, H. Z. Phys. Chem. 1999, 213 (II), 129.

[§] Dedicated to Professor R. W. Saalfrank on the occasion of his 60th birthday.

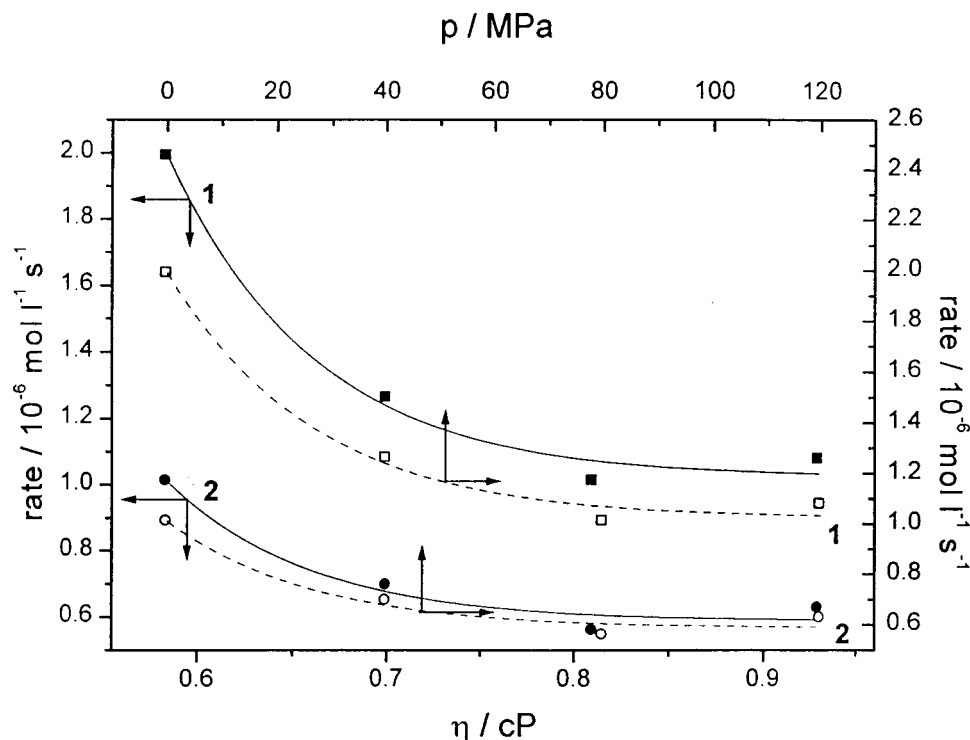
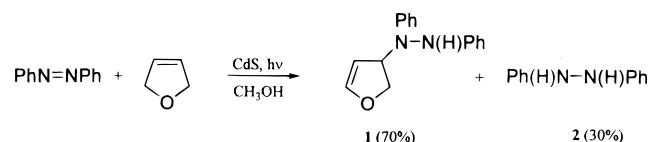


Figure 1. Reaction rates vs pressure or resulting viscosity.

SCHEME 1



adsorption onto CdS, SiO₂ supported CdS, and SiO₂ by NMR, measurement of adsorption constants, and application of the Hiemenz model.⁵ The second question was answered by attempts to scavenge the mutual radical cation by nucleophilic attack of the solvent. And finally, the third question was answered by studying the effect on high pressure on the reaction rate, a method applied the first time in semiconductor photocatalysis.

Results

Cadmium sulfide was prepared from sodium sulfide and an aqueous ammonia solution of cadmium sulfate (CdS-A) and SiO₂ supported CdS (CdS/SiO₂) analogously by stirring SiO₂ several hours in the cadmium sulfate solution before adding the sulfide. Reaction rates were measured by following the formation of **1** and **2** by HPLC. Unless otherwise noted, a pseudo-zero-order rate law was observed in both cases.

Influence of Pressure and Temperature. Irradiation of CdS/SiO₂, azobenzene, and 2,5-DHF in methanol/glycerol (1.1/1, v/v) decreased the rate of product formation as compared to methanol by 92% and the product ratio from **1**:**2** = 2.3 to 0.45.⁶ This suggested that the higher solvent viscosity may be responsible for the slower reaction. Accordingly, irradiation was performed at pressures from 0.1 to 120 MPa. A plot of reaction rates vs pressure or resulting viscosity⁷ revealed that both addition and reduction rates decrease with increasing pressure (Figure 1).

Both rates of addition (**1**) and reduction product (**2**) formation decreased exponentially with lowering the temperature from 50 to 15 °C, the former stronger than the latter. The corresponding Arrhenius plots are summarized in Figure 2.

Reactivity in Various Alcohols. When different linear alcohols were used in order to change the solvent viscosity, similar results were obtained as found for the temperature and high-pressure experiments (Figure 3).

Adsorption of Azobenzene and 2,5-DHF onto CdS-A, CdS/SiO₂ and Silica Gel. To obtain the adsorption constants of 2,5-DHF and azobenzene, the amount of adsorbed species was determined in methanol and aqueous solution at different initial concentrations after stirring the system overnight in the dark. The data were analyzed according to the Hiemenz model⁵ which assumes that solvent and solute compete for adsorption sites in a surface–solvent–solute monolayer. This model was already applied to the adsorption of alcohols onto TiO₂,⁸ of imines onto CdS,^{2b} and of 2,5-DHF onto ZnS.⁹ Initial concentrations of 2,5-DHF and azobenzene were in the range of $c_0 = 10^{-1}$ – 10^{-2} and $c_0 = 10^{-3}$ – 10^{-4} mol L⁻¹, respectively. A plot of equilibrium coverage n_{eq} as a function of remaining substrate concentration c_{eq} revealed in both cases the presence of a plateau and a linear increase at higher concentrations (Figure 4). From the plateau, the maximum surface concentration ($n_{\text{eq}}\text{max}$) of the adsorbate in the surface–solvent–solute monolayer is obtainable; from the slope and intercept of the plot of $c_{\text{eq}}(n_{\text{eq}})^{-1}$ vs c_{eq} , the adsorption constant and σ^0 , the average area covered per molecule in the solvent–solute monolayer can be extracted (Figure 4, Table 1).

Determination of the Pseudo-adsorption Constant of Azobenzene. The pseudo-adsorption constants of azobenzene were obtained for CdS-A and CdS/SiO₂ by measuring the initial rate as a function of azobenzene concentration. A recently published “in situ” method^{2b} accomplishes this in one single experiment, when the rate obeys a first-order law. This is the case at low concentrations of azobenzene, $c_0 \leq 2.3 \times 10^{-4}$ mol L⁻¹, at which the usually zero-order reaction becomes dependent on the concentration. The plot of reciprocal rates vs reciprocal concentrations^{10,11} results in a straight line (Figure 5), and from the slope (m) and intercept (b) the adsorption constant K_i =

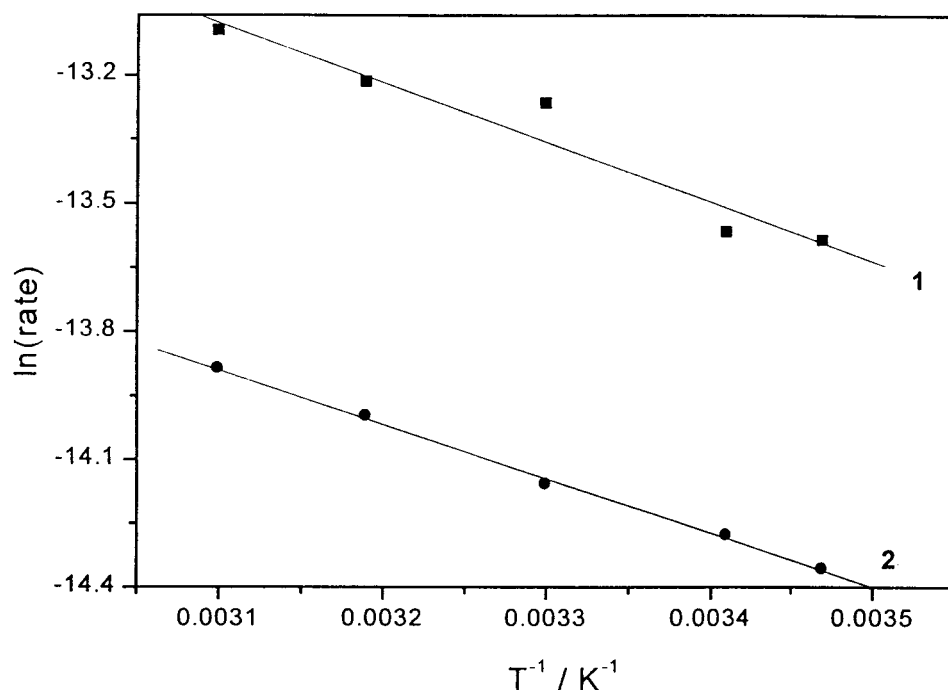


Figure 2. Arrhenius plots for the formation of 1 and 2.

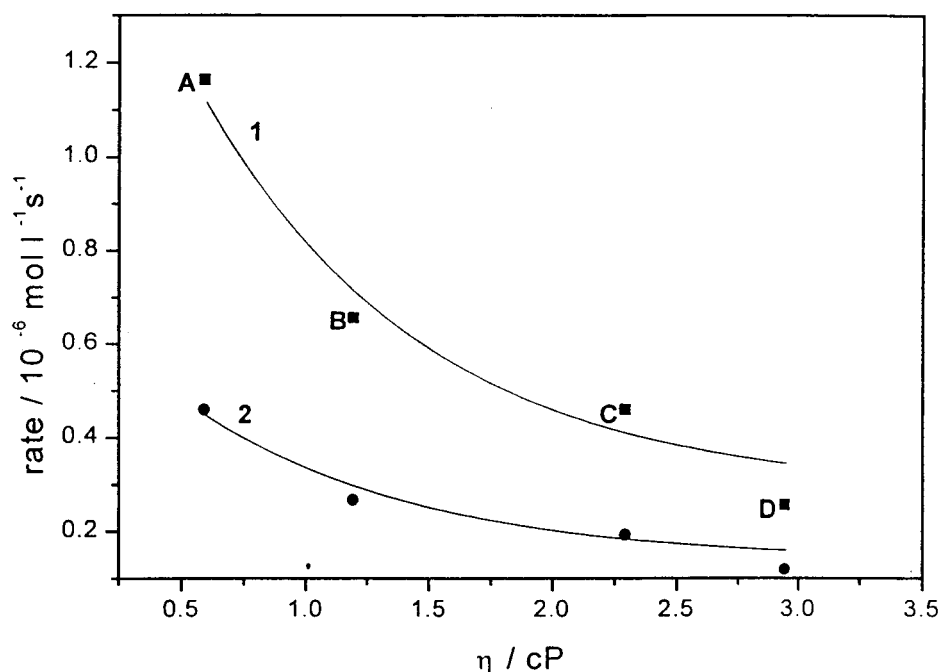


Figure 3. Reaction rates as a function of viscosity of alcoholic solvents: (A) MeOH; (B) EtOH; (C) 1-PrOH; (D) 1-BuOH.

$b(m)^{-1}$ is obtained as $1460 \pm 150 \text{ L mol}^{-1}$ and $2080 \pm 190 \text{ L mol}^{-1}$ for CdS-A and CdS/SiO₂, respectively.

Adsorption Studies by ¹³C NMR Spectroscopy. By analogy with NMR investigations of the adsorption of olefins onto ZnO,¹² 2,5-DHF was adsorbed from the gas phase onto the various powders and the ¹³C NMR spectrum was measured. Because of very long recording times, magnetic field instabilities arose, as indicated by a small highfield shift (−0.16 ppm) of TMS, and all the following values were therefore corrected for this. For all data, an experimental error of ± 0.2 ppm is realistic. For the adsorption of 2,5-DHF onto SiO₂, downfield shifts of 0.6 and 1.3 ppm for the olefinic and the α -carbon atoms, respectively, were measured (Table 2). In the case of CdS-A, the signal of the olefinic carbon atom remained almost

unchanged; that of the α -carbon atoms appeared 0.6 ppm downfield as compared to neat 2,5-DHF. Coadsorption of methanol had a significant effect only in the case of CdS-A. The adsorption shifts for the sp^3 and sp^2 carbon atoms in the presence of methanol increased by 0.8 and 0.9 ppm, respectively. For the adsorption of 2,5-DHF onto CdS/SiO₂, the olefinic and the α -carbon atoms were shifted to lower field by 1.1 and 1.8 ppm, respectively. In all cases, the distance between both signals of 2,5-DHF was 0.5–0.8 ppm smaller as compared to the neat sample.

Estimation of the Surface and Substrate Polarity with Reichardt's Dye. The polarity of the surfaces of CdS-A, CdS/SiO₂, and SiO₂ was estimated by measuring the long-wavelength solvatochromic absorption band of adsorbed Reichardt's dye.¹³

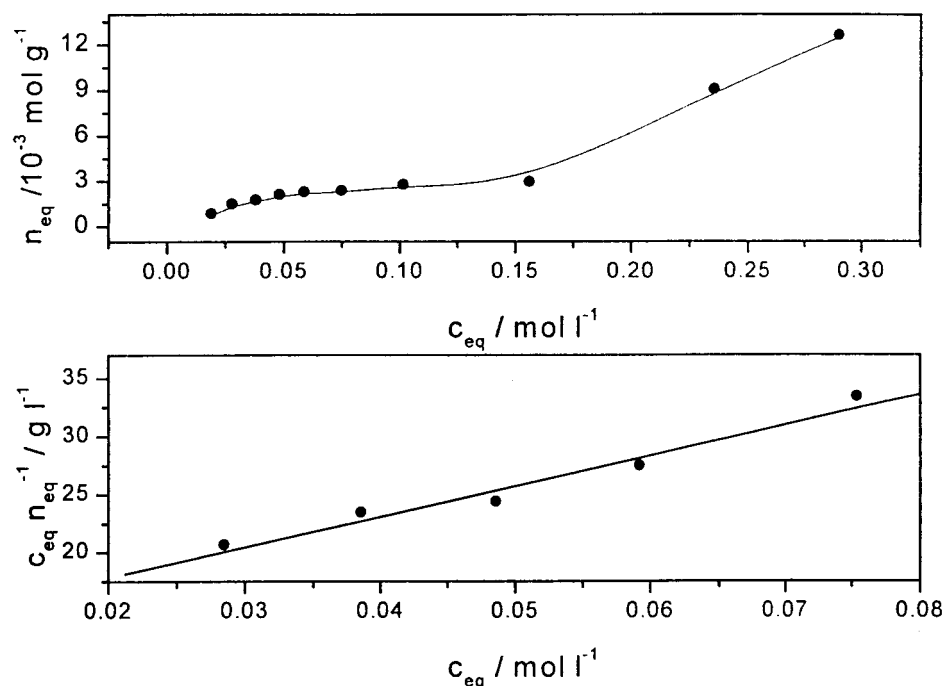


Figure 4. Adsorption of 2,5-DHF from aqueous solution onto CdS-A and Hiemenz linearization plot.

TABLE 1: Adsorption Data of 2,5-DHF^a

	A_{sp} [m ² g ⁻¹]	K_{ad} [L mol ⁻¹]		$(n_{eq})_{max}$ [mol g ⁻¹]		σ^o [nm ²]	
		A	B	A [10 ⁻³]	B [10 ⁻⁵]	A	B
CdS-A	157	18 ± 2	1130 ± 100	0.4 ± 0.1	0.7 ± 0.3	0.50 ± 0.05	27 ± 3
		21 ± 3 ^b		2.1 ± 0.2 ^b		0.07 ± 0.01 ^b	
CdS/SiO ₂	221	30 ± 1	1060 ± 220	1.6 ± 0.6	0.6 ± 0.1	0.20 ± 0.01	44 ± 1
SiO ₂	340	30 ± 2	1090 ± 260	1.3 ± 0.2	0.6 ± 0.1	0.35 ± 0.02	75 ± 5

^a A, 2,5-DHF; B, azobenzene. ^b In H₂O.

TABLE 2: ¹³C Chemical Shifts (δ [ppm]) of Neat 2,5-DHF, 2,5-DHF in Methanol, and 2,5-DHF Adsorbed onto CdS-A, CdS/SiO₂, and SiO₂ in the Absence and Presence of Co-Adsorbed Methanol

adsorbent/reference	C (sp ³)		C (sp ²)		CH ₃ OH	
	δ	$\Delta\delta^a$	δ	$\Delta\delta^a$	δ	$\Delta\delta^a$
2,5-DHF	75.6		127.0			
CH ₃ OH					49.9	
2,5-DHF/CH ₃ OH	76.0	0.4	127.0		49.9	
CdS-A/2,5-DHF	76.2	0.6	126.8	-0.2		
CdS-A					50.4	0.5
CdS-A/2,5-DHF/MeOH	77.4	1.4	127.7	0.7	51.1	1.2
CdS/SiO ₂ /2,5-DHF	77.4	1.8	128.1	1.1		
CdS/SiO ₂					51.6	1.7
CdS/SiO ₂ /2,5-DHF/MeOH	77.6	1.6	128.1	1.1	51.5	1.6
SiO ₂ /2,5-DHF	76.9	1.3	127.6	0.6		
SiO ₂					50.9	1.0
SiO ₂ /2,5-DHF/MeOH	77.4	1.4	127.9	0.9	51.4	1.5

^a Adsorption shifts relative to neat 2,5-DHF and CH₃OH.

For SiO₂, λ_{max} was directly observed at 490 ± 20 nm, while for CdS/SiO₂ and CdS-A the values of 535 ± 20 nm and 540 ± 20 nm were obtained from difference spectra, respectively (Figure 6). The polarity parameter $E_T(30)$ was calculated from the equation^{13a} $E_T(30) = 28592/\lambda_{max}$ and the obtained values were referenced to water ($E_T(30) = 63.1$ kcal mol⁻¹) and tetramethylsilane ($E_T(30) = 30.7$ kcal mol⁻¹) as extreme reference solvents in order to avoid non-SI units.¹⁴ The resulting E_T^N values for SiO₂, CdS/SiO₂ and CdS-A are 0.70 ± 0.06, 0.85 ± 0.07, and 0.68 ± 0.06, respectively. In homogeneous

2,5-DHF solution, Reichardt's dye exhibited a maximum at 764 nm, which corresponds to an E_T^N value of 0.37.

Discussion

Substrate Adsorption. Adsorption of gaseous cyclopentene onto SiO₂ is indicated by shifts of +0.7 and -0.8 ppm for the olefinic and α -carbon ¹³C NMR signals, respectively.¹² In the case of 2,5-DHF, corresponding shifts of +0.6 and +1.3 ppm were observed. The large downfield shift of the α -carbon signals in the latter case must be due to interaction between the oxygen atom and surface silanol groups. A corresponding weaker hydrogen bond to the C=C double bond is indicated by much smaller shifts of the olefinic signals. It is known that olefins adsorb onto the surface of silica through hydrogen-bonding.¹⁵ Coadsorption of methanol had only a negligible effect since the differences are within or very close to the experimental errors involved. This differs from 2,5-DHF adsorption onto CdS-A, where both signals experienced a much stronger downfield shift of 1.4 (α -C) and 0.7 (C=C) ppm in the presence, as compared to 0.6 and -0.2 ppm in the absence, of methanol, respectively. This suggests that the olefinic part interacts with adsorbed methanol since in homogeneous solution methanol affected only the chemical shift of the α -carbon signals (see Table 2). It is known that the adsorption of alcohols, ethers, and water onto silica occurs via hydrogen bonding as indicated by downfield shifts of the corresponding ¹³C NMR signals.^{16,17} Accordingly, adsorption shifts between 0.5 and 1.7 were observed for methanol which depend also on the presence of 2,5-DHF. In the case of the SiO₂ supported CdS-A, the data resemble those

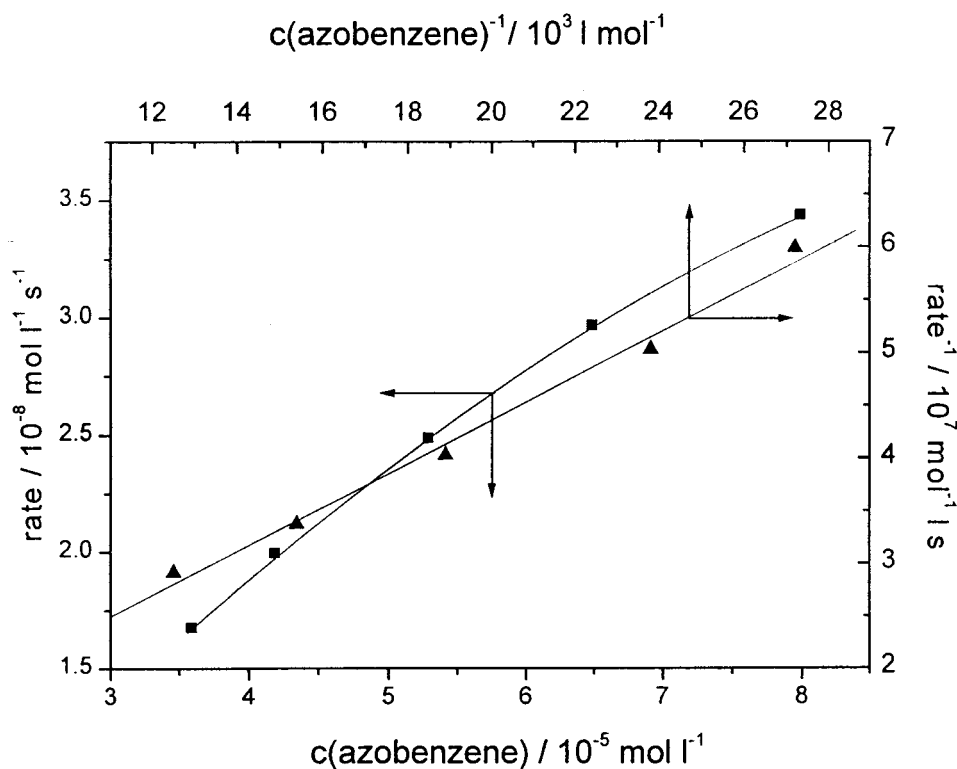


Figure 5. Dependence of the azobenzene disappearance rate on the initial concentrations and plot of reciprocal rates vs reciprocal concentrations.

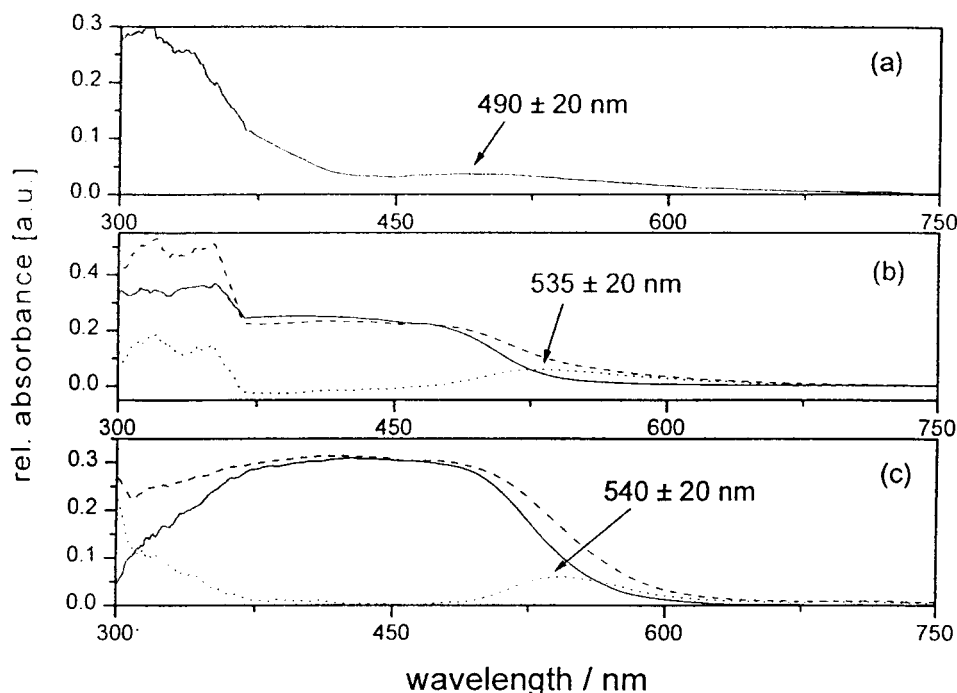


Figure 6. Diffuse reflectance spectra of adsorbed Reichardt's dye: (a) SiO_2 ; (b) CdS/SiO_2 ; (c) CdS-A ; (b and c) (\cdots) adsorbent and Reichardt's dye, (---) adsorbent; (—) difference spectra.

of unmodified SiO_2 and therefore suggest that adsorption of 2,5-DHF occurs primarily at the silica surface. In agreement with this conclusion is the fact that SiO_2 and CdS/SiO_2 afforded the same adsorption constant of 30 L mol^{-1} , which is about 50% larger as compared to CdS-A (vide infra). From these measurements, it is concluded that 2,5-DHF is adsorbed parallel to the cadmium sulfide surface.

For adsorption of 2,5-DHF onto SiO_2 , comparison of $n_{\text{eq(max)}} = 1.3 \times 10^{-3} \text{ mol g}^{-1}$ with the number of OH groups¹⁸ in amorphous silica ($4.6 \text{ nm}^{-2} \equiv 2.59 \times 10^{-3} \text{ mol g}^{-1}$)^{19,20} reveals

that about every second OH group is involved in the interaction with one 2,5-DHF molecule, in agreement with a flat adsorption as suggested by the ^{13}C NMR results. A similar estimation for the adsorption of 2,5-DHF onto CdS-A as based on the maximum surface concentration of $n_{\text{eq(max)}} = 0.4 \times 10^{-3} \text{ mol g}^{-1}$ and the maximum number of Cd^{2+} surface sites calculated for cubic CdS ,²¹ $1.54 \times 10^{-3} \text{ mol g}^{-1}$, reveals that 2,5-DHF is adsorbed at about every fourth Cd^{2+} center. Again, this is supported by the ^{13}C NMR results which revealed parallel adsorption also onto CdS-A . However, for both supports, the

presence of perpendicular adsorption cannot be excluded. Contrary to this, in the case of zinc sulfide (ZnS-B₁) 2,5-DHF occupies each Zn²⁺ site and σ^0 matches the calculated molecular area when adsorbed from aqueous solution.⁹ The difference can be rationalized by comparing the polarities of the two sulfides with those of 2,5-DHF and the solvents employed. Since the surface polarity of CdS-A ($E_T^N = 0.68 \pm 0.06$) is comparable with the value of methanol ($E_T^N = 0.762$),¹⁴ but is much higher than that of 2,5-DHF ($E_T^N = 0.366$),²² displacement of MeOH_{ad} by 2,5-DHF should be disfavored. Contrary to that, the highly polar solvent water ($E_T^N = 1.0$)¹⁴ is displaced completely from the less polar ZnS surface ($E_T^N = 0.57^{23}$) by the less polar 2,5-DHF. This explanation is corroborated by the data obtained for 2,5-DHF when it is adsorbed onto CdS-A from aqueous solution. In this case comparison of the maximum surface concentration of $n_{\text{eq(max)}} = 2.1 \pm 0.2 \times 10^{-3} \text{ mol g}^{-1}$ with the calculated maximum number of Cd²⁺ surface sites reveals that about every Cd²⁺-center is occupied by 2,5-DHF. The σ^0 value of $0.07 \pm 0.01 \text{ nm}^2$ matches quite well the molecular area of 0.09 nm^2 ²⁴ calculated for a perpendicular adsorbed molecule. The change to the more polar solvent water enables an almost 5-fold higher surface coverage of CdS-A. For CdS/SiO₂, the maximum surface concentration of 2,5-DHF ($1.6 \times 10^{-3} \text{ mol g}^{-1}$) is about the sum of the values for CdS-A ($0.4 \times 10^{-3} \text{ mol g}^{-1}$) and SiO₂.

The considerations outlined above are substantiated further by the σ^0 values obtained from Hiemenz plots. The area covered by a 2,5-DHF molecule in the saturated surface-solute-monolayer, is found to be 0.50 ± 0.05 , 0.35 ± 0.02 , and $0.20 \pm 0.01 \text{ nm}^2$ for CdS-A, SiO₂, and CdS/SiO₂, respectively, and differs not too much from the area of 0.21 nm^2 as calculated for an unsolvated molecule adsorbed parallel to the surface.²⁵ This qualitative agreement with the conclusions drawn from the maximum numbers of metal ion sites strongly suggests that 2,5-DHF adsorbs at surface [OH] or [SH] groups via hydrogen bonding.

Inspection of Table 1 reveals that the adsorption constants of 2,5-DHF onto SiO₂ and CdS/SiO₂ are equal. This suggests predominant adsorption on the SiO₂ support in the latter case. The better adsorption onto CdS/SiO₂ ($K_{\text{ad}} = 30 \pm 1 \text{ L mol}^{-1}$) as compared to CdS-A ($K_{\text{ad}} = 18 \pm 2 \text{ L mol}^{-1}$) is connected with a faster reaction and a higher product ratio of 1:2. The former increases by a factor of 2, while the latter increases from 0.9 to 2.1. Since the amount of azobenzene adsorbed is the same for both photocatalysts, it is likely that the higher 2,5-DHF surface concentration induced by SiO₂ increases also the amount of 2,5-dihydrofuryl radicals adsorbed at CdS and therefore accelerates C–N coupling with the PhN–NHPh radicals. Contrary to the result for imine adsorption onto cadmium sulfide, but analogous to the adsorption of 2,5-DHF onto ZnS,⁹ the pseudoadsorption constants of azobenzene as measured for CdS-A and CdS/SiO₂ by the in situ method^{2b} compare well with the genuine constants.

In comparison to 2,5-DHF, the maximum surface concentration $n_{\text{eq(max)}}$ for azobenzene of about $10^{-5} \text{ mol g}^{-1}$ is 2 orders of magnitude lower, whereas the adsorption constants are much higher and do not depend on the nature of the adsorbent. Comparison of the σ^0 values (Table 1) with the area covered by a flat, unsolvated molecule (0.52 nm^2)²⁶ reveals that the area covered by azobenzene on CdS-A, CdS/SiO₂, and SiO₂ is 52, 85, and 145 times higher than expected. Only at every 220th Cd²⁺ site of CdS-A an azobenzene molecule seems to be adsorbed. Depending on the adsorbent, only 0.7–2% of the surface area is covered, which suggests that the more polar methanol ($\mu = 1.7 \text{ D}^{22b}$) efficiently competes with the less polar

trans-azobenzene²⁷ ($\mu_{\text{trans}} \approx 0 \text{ D}$) for adsorption sites. Similar results were obtained for the imine adsorption onto CdS.^{2b} Together with the independence of the adsorption constant on the nature of the adsorbent, these results suggest that adsorption occurs not via hydrogen-bonding but rather through interaction with Brønsted acid sites.²⁸ In this case, the independence of the adsorption constant on the adsorbent can be rationalized since CdS and SiO₂ have similar pK_s values (6.1, 9.0,²⁹ and 6–8,³⁰ respectively) and CdS-A, CdS/SiO₂, and SiO₂ have two surface centers of similar pH values, respectively.³¹

Formation of Allyl Radicals. When OH radicals are generated by photolysis of H₂O₂ in the presence of 2,5-DHF formation of 3-hydroxytetrahydrofuran is observed.³² This may also occur in the CdS-catalyzed photoreaction via OH radicals produced by hole oxidation of water at surface CdO centers (eq 6).³³ However, no 3-hydroxytetrahydrofuran could be detected, even after complete consumption of azobenzene, whereas this was possible in a reference experiment when H₂O₂ was photolyzed. Furthermore, the CdS-A catalyzed photoreaction of azobenzene with 2-propanol afforded only hydrazobenzene and other products but no pinacol, the dimer of the expected 2-hydroxypropyl radical produced through H-abstraction by OH[•]. Furthermore, loading of CdS-A with 1% CdO completely inhibited the reaction.³⁴ Therefore, the involvement of OH[•] radicals in the oxidative reaction part is very unlikely.

Since existence of surface sulfur radicals at the illuminated CdS surface was recently supported by ESR experiments,³⁵ the 2,5-dihydrofuryl radicals may be formed through hydrogen abstraction by these radicals via the second “indirect” oxidation mechanism. (eqs 4, 5). To test this possibility, neat 1,4-dioxane or THF were used instead of 2,5-DHF in the CdS catalyzed photoreaction. The corresponding addition products were obtained, but the reaction became much slower. Assuming that the surface bound sulfur radical $-\text{S}^{\bullet}$ reacts like a dissolved methanethiyl radical, only unsaturated cyclic ethers should be reactive.³⁶ However, since 1,4-dioxane and THF gave the expected products, the indirect oxidation mechanism can be excluded for these saturated substrates, although it may operate in the case of the unsaturated ones.

Positive experimental evidence was found in favor of the direct oxidation of 2,5-DHF via dissociative electron transfer. Although it is known that radical cations are easily attacked by nucleophilic solvents such as methanol,³⁷ no corresponding side products could be detected in the CdS-catalyzed photoreactions of 2,5-DHF, 1-phenylcyclohexene, or α -pinene. The two latter olefins were selected since 1-phenylcyclohexene is known to form a relatively long-lived ($t_{1/2} \approx 50 \text{ ns}$) radical cation³⁸ and the α -pinene radical cation irreversibly cleaves to a distonic radical cation, in which nucleophilic attack by methanol is highly favored.³⁷ In control experiments, 1-phenylcyclohexene ($E_{\text{ox}} = 1.62 \text{ V}^{38}$) and α -pinene ($E_{\text{ox}} = 1.65 \text{ V}^{39}$) were added to a methanol solution of cerium(IV) ammonium nitrate ($E_{\text{ox}} = 1.28\text{--}1.74 \text{ V}^{40}$). The concomitant color change from red–orange to pale yellow occurred immediately in the former, but only 15 min later in the latter case. Analysis by FD mass spectroscopy revealed the presence of a methanol reaction product only for the 1-phenylcyclohexene experiment as indicated by a peak at $m/z = 190$ assignable to 2-methoxy-1-phenylcyclohexane, formed by nucleophilic attack of methanol on the intermediate radical cation of 1-phenylcyclohexene. Since no change of color was observed when methanol was added to cerium(IV) ammonium nitrate, a prior oxidation of methanol under formation of hydroxymethyl radicals does not take place. Therefore, the consecutive formation of the isomeric 2-hydroxymethyl-1-

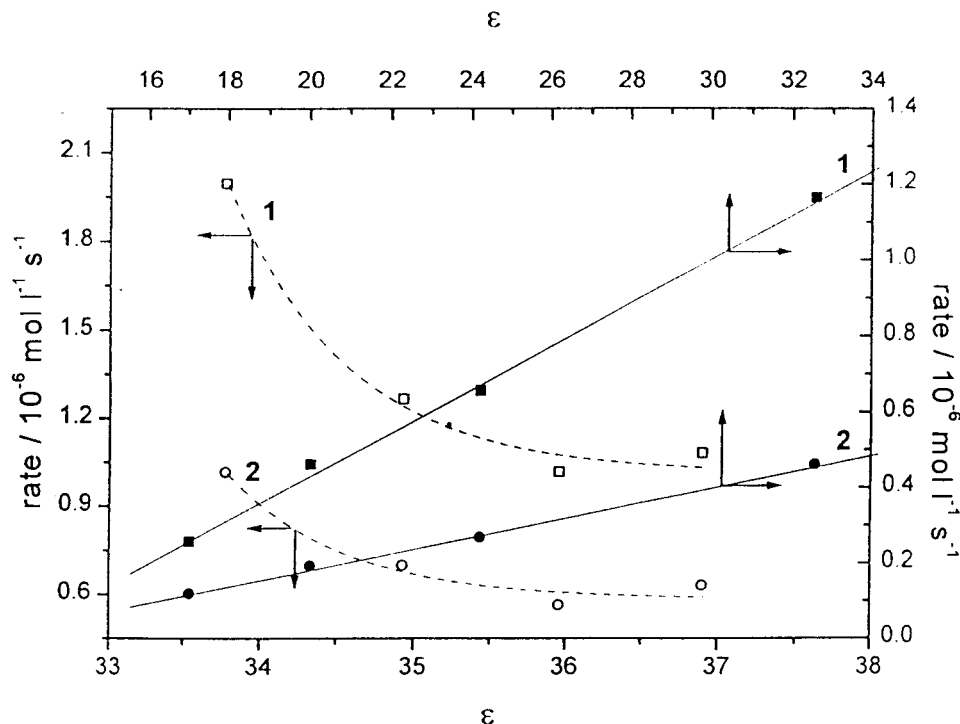


Figure 7. Reaction rates as a function of dielectric constant: (---) pressure experiments; (—) alcoholic solvents.

phenylcyclohexane by addition of hydroxymethyl radicals to 1-phenylcyclohexene, followed by H-abstraction from 1-phenylcyclohexene, can be excluded.

There is good evidence that the formation of 3-methoxycyclohexene and 1,2-dimethoxycyclohexene by electrochemical oxidation of cyclohexene in methanol proceeds through an initial two-electron oxidation to the corresponding carbenium ion.⁴¹ To favor this two-electron process also in the photoreaction, CdS-A was loaded with 3 wt % of ruthenium(IV)oxide hydrate which is known to be an excellent redox catalyst.⁴² When the resulting CdS-A/RuO₂ was employed as the photocatalyst in the reactions of 2,5-DHF and 1-phenylcyclohexene, only the addition products and hydrazobenzene could be detected by HPLC. However, FD-MS analysis in both cases revealed formation of a new side product ($m/z = 284$) which could have been formed by C–N coupling between the PhNH–NPh and 3-hydroxymethyltetrahydrofuryl radicals. Apparently, the presence of RuO₂ enables the oxidation of methanol to the hydroxymethyl radical and a proton. Addition to 2,5-DHF would afford the 3-hydroxymethyltetrahydrofuryl radical. Thus, contrary to the homogeneous reaction with cerium(IV), the photooxidation of methanol is possible in the presence of CdS-A/RuO₂. Attack of methanol on the mutual 2,5-dihydrofuryl cation formed by two-hole oxidation ($m/z = 282$) was not detected. When 1-phenylcyclohexene was employed as the olefin, 2-hydroxymethyl-1-phenylcyclohexane ($m/z = 190$) was observed. This indicates that the intermediary 2-hydroxymethyl-1-phenylcyclohexyl radical abstracts hydrogen from 1-phenylcyclohexene and methanol but does not couple with the PhNH–NPh radical as observed in the case of 2,5-DHF. This difference is in accordance with a much higher steric hindrance of C–N coupling for the 2-hydroxymethyl-1-phenylcyclohexyl as compared to the 3-hydroxymethyltetrahydrofuryl radical.⁴³

The failure to detect any products arising from nucleophilic attack of the solvent on a mutual intermediate radical cation indicates that its lifetime is extremely short, or more likely that formation of the allyl radical occurs through a dissociative electron transfer. Although it is known that radical cations may

be very strong acids, the calculated pK_a value⁴⁴ for α -pinene of +1 signals that nucleophilic attack should be able to compete with deprotonation. This is less favored in the case of 2,5-DHF and 1-phenylcyclohexene for which pK_a values of –16 and –15 are calculated, respectively.

Pressure and Temperature Dependence. Although the decrease in formation rates for **1** and **2** in methanol at higher pressures points to a viscosity effect, a definite conclusion cannot be drawn since increasing pressure also increases the dielectric constant of the solvent.^{45,46} To differentiate between these two possibilities, the rates were measured in a series of alcohols for which viscosity and dielectric constant change in an opposite fashion. While the rates again decreased with increasing viscosity, they increased when plotted as a function of increasing dielectric constant (Figure 7). This indicates that the rate decrease at higher pressure must be due to a viscosity effect.

Activation volumes ΔV^\ddagger were obtained from the plots of $\ln(\text{rate})$ vs pressure (Figure 8) as $+17.4 \pm 3.4$ and $+15.8 \pm 2.3$ cm³ mol^{–1}, while activation energies of 11.6 ± 1.3 and 10.6 ± 0.9 kJ mol^{–1} were calculated from the Arrhenius plots (Figure 2) for the formation of **1** and **2**, respectively.

It is unlikely that the activation volume is connected with substrate adsorption or product desorption, since high pressure does not significantly affect the adsorption of noncharged substrates.⁴⁷ An influence on the interfacial electron transfer steps is also ambiguous, since contrary to homogeneous solution, where the rates of very fast electron transfer reactions can become diffusion controlled,⁴⁸ no parallel explanation is possible for the heterogeneous case since interfacial collision rates depend on molecular mass but not on diffusion rates.⁴⁹ Therefore, the activation volume measured for the formation of **1** may stem from the diffusion of the intermediate radicals to each other or from the subsequent C–N coupling step itself. The latter case can be excluded since bond formation between neutral organic species in homogeneous solution in general has a negative activation volume.^{50,51} The only exception is radical recombination in the termination step of polymerizations.⁵² These reactions possess ΔV^\ddagger values in the range of +13 to +25 cm³ mol^{–1} which

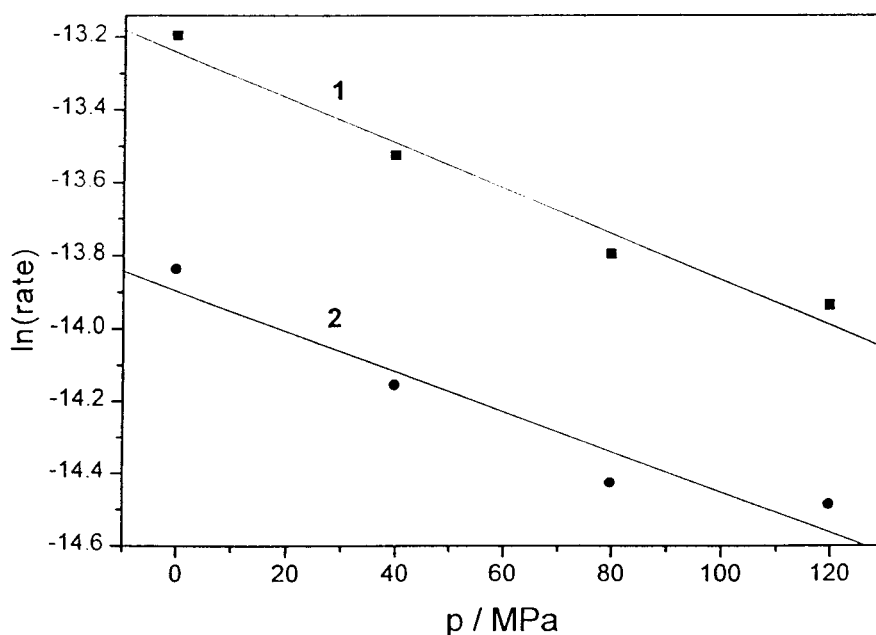


Figure 8. Plot of $\ln(\text{rate})$ vs pressure for the formation of **1** and **2**.

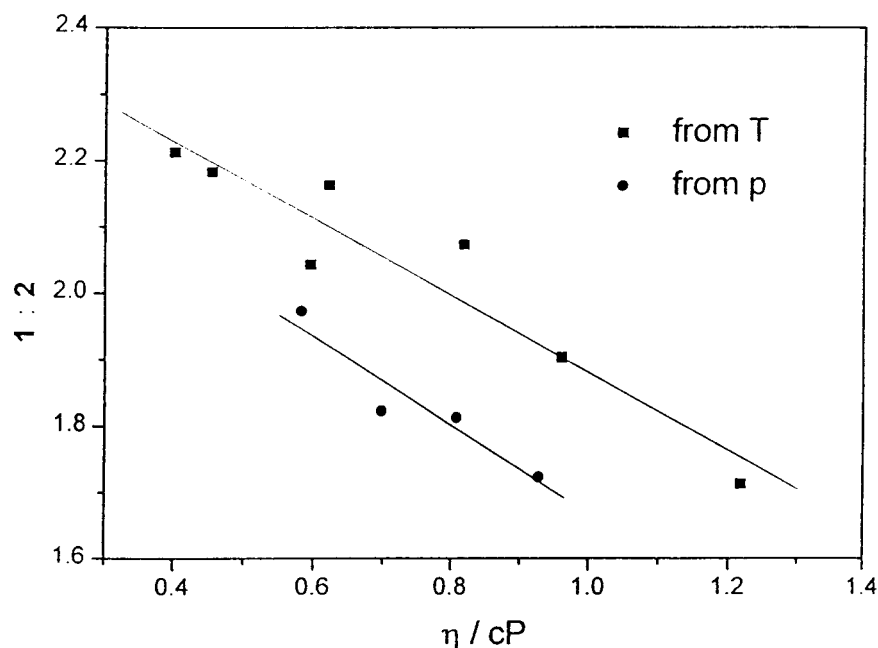


Figure 9. Dependence of product ratio **1:2** on solvent viscosity.

are composed of the large and positive contribution of diffusion and the small and negative part of radical C–C coupling. Hence, the activation volume found for **1** most likely originates primarily from diffusion of the intermediate radicals to each other and only to a minor part from C–N coupling and therefore should resemble the activation volume for the viscous flow of methanol. The fact that the latter value of $+8 \text{ cm}^3 \text{ mol}^{-1}$ ⁵³ is significantly smaller suggests that the radicals do not diffuse in the bulk homogeneous solution but in a solvent–solute–surface multilayer. This should result in a higher viscosity and consequently the activation volume should become more positive.

Since the same activation parameters as for **1** were also found for the formation of the reduction product **2**, the disproportionation pathway (eq 3), which involves radical diffusion, is highly favored. However, also the secondary reduction step (eq 2) may be partly involved as suggested by the smaller pressure effect

as compared to **1** (Figure 1). The conclusion that changes in solvent viscosity are responsible for the observed pressure and temperature effects is further corroborated by the same dependence of the product ratio **1:2**. Irrespective of whether the viscosity is calculated from the pressure or temperature experiments, a plot of the product ratio vs viscosity affords two straight lines with slopes identical within experimental error (-0.60 ± 0.06 and -0.70 ± 0.04 , Figure 9). When the different alcohols were used to change the viscosity, the product ratio also decreased with increasing viscosity.

Conclusion

From ^{13}C NMR and adsorption data, it is concluded that 2,5-DHF adsorbs onto cadmium sulfide through hydrogen bonding via surface [OH] and [SH] groups, while a Brønsted acid–base interaction is postulated for azobenzene. The absence of any

methanol addition products disfavors formation of an intermediate radical cation in the interfacial electron transfer to the reactive hole. It therefore is assumed that oxidation and deprotonation of 2,5-DHF to the dihydrofuryl radical is a concerted process. High-pressure experiments reveal that the reaction has a positive activation volume, which strongly suggests that not the C–N bond formation between the 2,5-dihydrofuryl and PhN–N(H)Ph radicals is rate determining but rather the diffusion of these intermediates within a surface–solvent–solute multilayer.

Experimental Section

All experiments were performed as described in refs 1 and 2c unless otherwise noted. MS represents a JEOL MStation 700 (EI 70 eV, FD 2 kV). Irradiations were performed with a 100 W tungsten halogen lamp in a solidex immersion lamp apparatus (method A) and with an Osram XBO 150 W xenon arc lamp (I_0 (400–520 nm) = 2.0×10^{-6} Einstein $\text{s}^{-1} \text{cm}^{-2}$) in a cylindrical 15 mL quartz cuvette, equipped with a cooling jacket and a Pyrex cutoff filter, on an optical train (method B). Samples were withdrawn every 15 min. Both apparatus were equipped with Teflon-coated magnetic stirring bars. In the temperature-dependent measurements, an additional 0.05 M CuCl_2 solution was used to absorb IR radiation. Every sample was thermostated for 30 min prior to irradiation; temperature was kept constant during the illumination through circulation of EtOH as a cooling liquid. Irradiations under pressure were performed in a thermostated (± 0.1 °C) high-pressure cell,⁵⁴ equipped with two windows. The sample suspensions were transferred into a “pillbox” optical cell⁵⁵ equipped with a Teflon-coated magnetic stirring bar. The pillbox was then placed in the high-pressure cell, which was filled with distilled water as the pressure-transmitting medium. After the adjustment of the desired pressure, the samples were thermostated for 15 min at 20 °C. Irradiations were carried out with a high-pressure mercury lamp (Osram HBO 100W/2). UV-light was cut off with a Pyrex filter. The values of ΔV^\ddagger were determined from plots of $\ln(\text{rate})$ vs pressure according to the equation $(\partial \ln(\text{rate})/\partial p)_T = -\Delta V^\ddagger/RT$. Unless otherwise noted, a standard procedure as described for the reaction of azobenzene with THF was followed in all experiments; under these experimental conditions, the reaction follows a zero order rate law.

CdS-A. To a solution of $\text{CdSO}_4 \cdot 8/3\text{H}_2\text{O}$ (25.7 g, 0.1 mol) in aqueous NH_3 (300 mL, 10%) 100 mL of a solution of $\text{Na}_2\text{S} \cdot \text{H}_2\text{O}$ (22.3 g, 0.1 mol) was added over a period of 1.5 h. The resulting yellow suspension was stirred for 20 h. After separation by suction filtration, the residue was washed with water to constant pH and dried over P_2O_5 in a desiccator. The ground orange powder was stored under N_2 . Micro analysis: CdS (144.47) calcd. S, 22.19; found S, 17.48; C, 0.27; H, 0.28; N, 0.00. Specific surface area: $157 \text{ m}^2 \text{g}^{-1}$ (BET, N_2). Particle size: 2–50 μm sized aggregates as determined by light scattering, which consist of 5–10 nm crystallites as determined by transmission electron microscopy.²⁸

CdS-A/RuO₂. CdS-A was ground in a mortar with 3 wt % of ruthenium(IV)oxide hydrate.

CdS/SiO₂. Silica gel (Grace type 432, neutral, specific surface area $340 \text{ m}^2 \text{g}^{-1}$) (10 g, 0.17 mol) and $\text{CdSO}_4 \cdot 8/3\text{H}_2\text{O}$ (4.34 g, 20.8 mmol) were stirred overnight in aqueous NH_3 (150 mL, 10%). $\text{Na}_2\text{S} \cdot \text{H}_2\text{O}$ (4.66 g, 20.8 mmol) dissolved in water (50 mL) was added dropwise within a period of 1.5 h. The resulting yellow suspension was stirred for 20 h and worked up as described for CdS-A. Micro analysis: CdS (144.47) calcd. S, 6.66; found S, 5.22; C, 0.59; H, 0.35; N, 0.01. Specific surface area: $221 \text{ m}^2 \text{g}^{-1}$ (BET, N_2).

Reaction of Azobenzene with THF (Standard Procedure). CdS-A (50 mg, 0.3 mmol) and a solution of azobenzene (31 mg, 0.17 mmol) in THF (15 mL) were suspended for 15 min by sonication under N_2 . Irradiation was performed by method B. The reaction was followed by HPLC. After 150 min of irradiation a small aliquot was withdrawn, CdS was filtered off through a micropore filter (pore size $> 0.2 \mu\text{m}$), and a mass spectrum was recorded. MS-FD: m/z 254 [M^+], inter alia.

Reaction of Azobenzene with Dioxane. CdS-A (250 mg, 1.5 mmol) and a solution of azobenzene (364 mg, 2 mmol) in dioxane (80 mL); method A, 16 h irradiation time. MS–FD m/z : 270 [M^+], inter alia.

Photolysis of H_2O_2 in the Presence of 2,5-DHF. 2,5-DHF (11.2 mL, 0.15 mol) and H_2O_2 p.a. (degassed, N_2) (0.8 mL, 7.2 mmol); method B, 3 h irradiation time. 3-hydroxytetrahydrofuran was detected by GC-MS: 100 °C, retention time = 2.0 min, MS-EI, m/z : 88.

Reaction of Azobenzene with 2,5-DHF. CdS-A (50 mg, 0.3 mmol) and a methanolic solution (14.7 mL) of azobenzene (31 mg, 0.17 mmol) were suspended by sonication for 15 min under N_2 . Thereafter, 2,5-DHF (0.3 mL, 4.1 mmol) was added. Irradiation (method B) for 3 h (complete consumption of azobenzene). GC-MS, 100 °C, no peak at retention time = 2.0, MS-EI (70 eV); m/z 88 not found.

Reaction of Azobenzene with 2-Propanol. CdS-A (50 mg, 0.3 mmol) and a methanolic solution (14.7 mL) of azobenzene (31 mg, 0.17 mmol) were suspended by sonication for 15 min under N_2 . Thereafter, 2-propanol (0.3 mL, 4.1 mmol) was added and irradiation was performed by method B for 140 min. MS-FD m/z : 182, 184, 252, 284.

Reaction of Cerium(IV)Ammonium Nitrate with 1-Phenylcyclohexene. Cerium(IV)ammonium nitrate (1.37 g, 2.5 mmol) was dissolved in methanol (14.6 mL). After addition of 1-phenylcyclohexene (0.4 mL, 2.5 mmol) an immediate color change of the solution from deep red–orange to pale yellow was observed and the olefin was completely consumed. Extraction of the solution with chloroform and removal of the solvent led to a blue–green oil. MS-FD m/z : 190 [M^+], inter alia.

Reaction of Cerium(IV)Ammonium Nitrate with α -Pinene. Cerium(IV)ammonium nitrate (1.37 g, 2.5 mmol) was dissolved in methanol (14.6 mL). After addition of α -pinene (0.4 mL, 2.5 mmol), the color changed from deep red–orange to pale yellow. After 15 min, consumption of the olefin was complete. A MS-FD spectrum of the reaction solution was recorded, m/z : 166 [M^+], inter alia.

Reaction of Azobenzene with 1-Phenylcyclohexene. CdS-A (50 mg, 0.3 mmol) and a methanolic solution (14.34 mL) of azobenzene (31 mg, 0.17 mmol) were suspended by sonication for 15 min under N_2 . Thereafter, 1-phenylcyclohexene (0.66 mL, 4.1 mmol) was added and irradiation was performed by method B for 60 min. MS-FD m/z : 340 [M^+], inter alia.

Reaction of Azobenzene with α -Pinene. CdS-A (50 mg, 0.3 mmol) and a methanolic solution (14.35 mL) of azobenzene (31 mg, 0.17 mmol) were suspended by sonication for 15 min under N_2 . After addition of α -pinene (0.65 mL, 4.1 mmol), the suspension was irradiated for 60 min by method B. MS-FD m/z : 318 [M^+], inter alia.

Reaction of Azobenzene with 2,5-DHF in the Presence of CdS-A/RuO₂. CdS-A/RuO₂ (51.7 mg, 0.3 mmol) and a methanolic solution (14.7 mL) of azobenzene (31 mg, 0.17 mmol) were suspended by sonication for 15 min under N_2 . Thereafter, 2,5-DHF (0.3 mL, 4.1 mmol) was added and irradiation was performed by method B for 60 min. MS-FD m/z : 284 [M^+], 182, 184, 252, 273, 320, 352.

Reaction of Azobenzene with 1-Phenylcyclohexene in the Presence of CdS-A/RuO₂. As described above, except that 1-phenylcyclohexene (0.66 mL, 4.1 mmol) was added and irradiation was performed for 180 min. MS-FD m/z : 190 [M^+], 157, 184, 314, 340.

Reaction of 2,5-DHF with Azobenzene under Various Conditions. In *Methanol/Glycerol*. CdS/SiO₂ (150 mg, 0.31 mmol) and a methanolic solution (7.7 mL) of azobenzene (46 mg, 0.25 mmol) were suspended for 15 min by sonication under N₂. After that, glycerol (7 mL) was added and the suspension was sonicated for further 15 min. Finally, 2,5-DHF (0.3 mL, 4.1 mmol) was added, method B, 60 min irradiation time. Samples were withdrawn every 15 min and analyzed by HPLC.

Pressure Dependence (Standard Procedure). CdS/SiO₂ (300 mg, 0.62 mmol) and a methanolic solution (29.4 mL) of azobenzene (62 mg, 0.34 mmol) were suspended for 15 min by sonication under N₂. Thereafter, 2,5-DHF (0.6 mL, 8.2 mmol) was added. An amount of 3 mL of this suspension, stored under stirring in the dark, was sonicated for 2 min, filled into the pillbox, and illuminated for 10, 20, 30, or 40 min under variable pressures (1–1200 bar). Samples were withdrawn every 15 min and analyzed by HPLC. The reported activation volumes are the average of two experiments.

Temperature Dependence. CdS/SiO₂ (150 mg, 0.31 mmol) and a methanolic solution (14.7 mL) of azobenzene (31 mg, 0.17 mmol) were suspended for 15 min by sonication. Thereafter, 2,5-DHF (0.3 mL, 4.1 mmol) was added and irradiation was performed by method B for 60 min at different temperatures (–22 to 50 °C). The reaction was followed by HPLC. The reported activation energies are mean values of two experiments.

Solvent Dependence. As described above except using 14.7 mL of ethanol, 1-propanol, and 1-butanol.

Competition Experiment. CdS-A (200 mg, 1.2 mmol) and a methanolic solution (14.25 mL) of azobenzene (31 mg, 0.17 mmol) were suspended by sonication for 15 min under N₂. After addition of 2,5-DHF (0.05 mL, 0.7 mmol) the suspension was irradiated for 30 min by method B. Thereafter, 1-phenylcyclohexene (0.7 mL, 4.1 mmol) was added and irradiation was continued for further 60 min. HPLC-analysis, MS-FD, m/z : 252, 340, 138, and 314, corresponding to the addition product of 2,5-DHF, 1-phenylcyclohexene, and the olefin hydrodimer, respectively.

Adsorption of 2,5-DHF onto CdS/SiO₂. A methanolic suspension (15 mL) of CdS/SiO₂ (150 mg, 0.31 mmol) adjusted to different concentrations c_0 of 2,5-DHF (0.02–0.3 mol L^{–1}) was sonicated for 5 min and stirred at room temperature (20 ± 3 °C) overnight in the dark. CdS/SiO₂ was filtered off through a micropore filter (pore size > 0.2 μm), and c_{eq} was determined by HPLC analysis. The amount of adsorbed 2,5-DHF was referred to 1 g of CdS/SiO₂ (n_{eq}). In addition to the measured n_{eq} values, calculated values were obtained through curve fitting in the concentration range from 1 × 10^{–2} to 1 × 10^{–1} mol L^{–1}.

Adsorption of 2,5-DHF onto CdS-A. As described above but using a methanolic or aqueous suspension of CdS-A (150 mg, 1.1 mmol) instead of CdS/SiO₂.

Adsorption of 2,5-DHF onto Silica Gel (Grace, type 432). As described above but using SiO₂ (105 mg, 1.7 mmol) instead of CdS/SiO₂.

Adsorption of Azobenzene onto CdS/SiO₂. As described above but using CdS/SiO₂ (200 mg, 0.41 mmol) and different concentrations c_0 of azobenzene (0.3 to 12.8 mmol L^{–1}). In addition to the measured n_{eq} values, calculated values were obtained through curve fitting in the concentration range from 1 × 10^{–3} to 5 × 10^{–3} mol L^{–1}.

Adsorption of Azobenzene onto CdS-A. As described above but using CdS-A (100 mg, 0.6 mmol).

Adsorption of Azobenzene onto Silica Gel (Grace, type 432). As described above but using SiO₂ (200 mg, 3.2 mmol).

Dependence of Rate on Azobenzene Concentration (“In Situ” Method^{2b}). CdS-A (50 mg, 0.3 mmol) or CdS/SiO₂ (150 mg, 0.31 mmol) and a solution of azobenzene (0.41 mg, 0.23 mmol) in methanol (14.7 mL) were sonicated for 15 min. Thereafter, 2,5-DHF (0.3 mL, 4.1 mmol) was added and irradiation was performed by method B (additional 400 nm cutoff filter) for 140 min. Every 15 min a sample was withdrawn and analyzed by HPLC. From the concentration vs time curve the rate was determined by construction of a tangent at a given concentration.

¹³C NMR Spectra of Adsorbed Substrates. A dried NMR tube was filled with the sample powder (CdS-A, CdS/SiO₂, SiO₂) (1 g) and evacuated several times. Thereafter, the adsorbate (2,5-DHF, methanol or methanol/2,5-DHF) was introduced via the vapor phase. This procedure was repeated nine times. ¹³C NMR spectra were recorded at room temperature.¹² A susceptibility correction of the chemical shifts of 0.155 ppm was applied, based on the upfield shift of –0.155 ppm as observed for TMS physisorbed onto CdS-A. The obtained spectra were compared to that of neat 2,5-DHF or methanol, measured in the presence of TMS.

Estimation of the Surface Polarity. To a solution of Reichardt’s dye (0.6 mg, 1 μmol) in dichloromethane (2.5 mL) CdS-A, CdS/SiO₂, or SiO₂ (200 mg, 1.2, 0.41, or 3.2 mmol) were added. After 15 min of sonication, the solvent was removed and the powder was dried for 10 min in vacuo. Thereafter, the diffuse reflectance UV–vis spectrum of the adsorbed dye was measured. The E_T^N value was calculated according to $E_T^N = (E_T - 30.7)/32.4$.¹⁴

Acknowledgment. This work was supported by Volkswagen-Stiftung and Fonds der Chemischen Industrie. We thank Prof. G. Emig for specific surface area determinations, Grimm Labortechnik for particle size determinations, and Dr. C. Dücker-Benfer for assistance with the high-pressure experiments.

References and Notes

- (1) Künne, R.; Feldmer, C.; Knoch, F.; Kisch, H. *Chem.—Eur. J.* **1995**, *1*, 441.
- (2) (a) Schindler, W.; Knoch, F.; Kisch, H. *Chem. Ber.* **1996**, *129*, 925. (b) Schindler, W.; Kisch, H. *J. Photochem. Photobiol. A: Chem.* **1997**, *103*, 257. (c) Keck, H.; Schindler, W.; Knoch, F.; Kisch, H. *Chem.—Eur. J.* **1997**, *3*, 1638.
- (3) Schindler, W.; Kisch, H. Unpublished.
- (4) Jin, Z.; Li, Q.; Zheng, X.; Xi, C.; Wang, C.; Zhang, H.; Feng, L.; Wang, H.; Chen, Z.; Jiang, Z. *J. Photochem. Photobiol. A: Chem.* **1993**, *71*, 85.
- (5) Hiemenz, P. C. *Principles of Colloidal and Surface Chemistry*, 2nd ed.; M. Decker: New York, 1986.
- (6) The reaction rates of **1** and **2** decreased by 96% and 84%, respectively.
- (7) Weber, W. *Rheol. Acta* **1975**, *14*, 1012.
- (8) (a) Cunningham, J.; Srijaranai, S. *J. Photochem. Photobiol. A: Chem.* **1991**, *58*, 361. (b) Cunningham, J.; Sedláč, P. *J. Photochem. Photobiol. A: Chem.* **1994**, *77*, 255. (c) Cunningham, J.; Al-Sayyed, G. *J. Chem. Soc., Faraday Trans.* **1990**, *86*, 3935.
- (9) Hörner, G.; Johne, P.; Künne, R.; Twardzik, G.; Kisch, H. *Chem.—Eur. J.* **1999**, *5*, 208.
- (10) Mills, A.; Williams, G. *J. Chem. Soc., Faraday Trans. 1* **1987**, *83*, 2647.
- (11) Al-Ekabi, H.; de Mayo, P. *Tetrahedron* **1986**, *42*, 6277.
- (12) Ali, I. T.; Gay, I. D. *J. Phys. Chem.* **1981**, *85*, 1251.
- (13) (a) Michels, J. J.; Dorsey, J. G. *Langmuir* **1990**, *6*, 414. (b) Tavener, S. J.; Clark, J. H.; Gray, G. W.; Heath, P. A.; Macquarrie, D. *J. Chem. Commun.* **1997**, 1147.
- (14) Reichardt, C. *Solvents and Solvent Effects in Organic Chemistry*, 1st ed.; VCH: Weinheim, 1988; p 364.

- (15) Iler, R. K. *The Chemistry of Silica*; John Wiley: New York, 1979; p 648.
- (16) Ponc, V.; Knor, Z.; Cerný, S. *Adsorption on Solids*; Butterworths: London, 1974.
- (17) (a) Kalinowski, H. O.; Berger, S.; Braun, S. *¹³C NMR-Spektroskopie*; Georg Thieme Verlag: Stuttgart, New York, 1984. (b) Stothers, J. B. *Carbon-13 NMR Spectroscopy*; Academic Press: New York, London, 1972. (c) Günther, H. *NMR-Spektroskopie*; Georg Thieme Verlag: Stuttgart, New York, 1984.
- (18) Calculation was carried out analogous to ref 21, assuming a hexagonal quartz structure.
- (19) Hiemstra, T.; van Riemsdijk, W. H. *J. Colloid. Interface Sci.* **1989**, *136*, 132.
- (20) Calculated for a specific surface area of 340 m² g⁻¹ of the silica used in this work.
- (21) (a) Calculated from the structural data of cubic CdS^b for a specific surface area of 157 m² g⁻¹. Chan, D.; Perram, J. W.; White, L. R.; Healy, T. W. *J. Chem. Soc., Faraday Trans. 1* **1975**, 1046. (b) Data from ASTM-card-index.
- (22) (a) From comparison with the dipole moments of THF, 2,5-DHF, and furan (1.63, 1.59, and 0.66 D^b, respectively) one would expect, however, that the E_T^N value of 2,5-DHF should be in the range of 0.164 to 0.270, corresponding to furan and THF, respectively. (b) See: Lide, D. R.; Raton, H. P. R. *Handbook of Chemistry and Physics*, 75th ed.; CRC Press: Boca Raton, 1994.
- (23) Hörner, G.; Kisch, H. Unpublished.
- (24) Estimated from a molecular model as 0.24 nm × 0.38 nm.
- (25) Estimated from a molecular model as 0.46 nm × 0.45 nm.
- (26) Estimated from a molecular model as 1.08 nm × 0.48 nm.
- (27) Since in the dark adsorption experiments light could not be completely excluded, *cis*-azobenzene was present in about 1%.
- (28) Reinheimer, A.; Fernández, A.; Kisch, H. *Z. Phys. Chem.* **1999**, *213* (II), 129.
- (29) Park, S. W.; Huang, C. P. *J. Colloid. Interface Sci.* **1987**, *117*, 431.
- (30) Bandosz, T. J.; Lin, C.; Ritter, J. A. *J. Colloid. Interface Sci.* **1998**, *198*, 347.
- (31) Reinheimer, A.; Kisch, H. Unpublished.
- (32) Zeug, N.; Bücheler, J.; Kisch, H. *J. Am. Chem. Soc.* **1985**, *107*, 1459.
- (33) The XRD-pattern obtained for CdS-A exhibits broad peaks which may be due to the presence of oxide or hydroxide species at the surface of the sample. This effect is confirmed by the XPS analysis of the sample. CdS-A shows compared to commercial, inactive CdS a higher heterogeneity of oxygen species. The valence band edge of CdO is located at 2.4 V, and therefore formation of OH radicals ($E_{OX}(OH^-/OH^*) = +2.4$ V) may occur according to eq 6.
- (34) Endres, U.; Kisch, H. Unpublished.
- (35) (a) Anpo, M.; Matsumoto, A.; Kodama, S. *J. Chem. Soc., Chem. Commun.* **1987**, 1038. (b) Nakaoka, Y.; Nosaka, Y. *J. Phys. Chem.* **1995**, *99*, 9893. (c) Kamat, P. V.; Dimitrijevic, N. M.; Fessenden, R. W. *J. Phys. Chem.* **1987**, *91*, 396.
- (36) Lunazzi, L.; Placucci, G.; Grossi, L. *Tetrahedron* **1983**, *39*, 159.
- (37) Du, X.; Arnold, D. R.; Boyd, R. J.; Shi, Z. *Can. J. Chem.* **1991**, *69*, 1365.
- (38) Kojima, M.; Kakehi, A.; Ishida, A.; Takamuku, S. *J. Am. Chem. Soc.* **1996**, *118*, 2612.
- (39) Shono, T.; Ikeda, A. *J. Am. Chem. Soc.* **1972**, *94*, 7892.
- (40) Aylward, G. H.; Findlay, T. J. V. *Datensammlung Chemie in SI-Einheiten*, 2nd ed.; VCH: Weinheim, 1986.
- (41) Yoshida, K.; Kanbe, T.; Fueno, T. *J. Org. Chem.* **1977**, *42*, 2313.
- (42) Miles, H. H. *J. Electroanal. Chem. Interfacial Electrochem.* **1975**, *60*, 84.
- (43) The alternative, that the byproduct is the isomeric 2-methoxy-1-phenylcyclohexene is unlikely. Since its formation occurs by solvent attack on the radical cation, as demonstrated in the homogeneous reaction with cerium(IV), it already should have been formed in the photoreaction with unmodified CdS-A.
- (44) From the standard redox potential (E_{OX} for 2,5-DHF, 1-phenylcyclohexene, and α -pinene is 2.70, 2.67, and 1.71 V, respectively) and the standard free energy for gas-phase bond dissociation of the allylic CH bond ΔG°_{BDE} (78 kcal mol⁻¹), the pK_A value can be estimated following: Dinnocenzo, J. P.; Banach, T. E. *J. Am. Chem. Soc.* **1989**, *111*, 8646.
- (45) Schäfer, K. *Landolt-Börnstein, Zahlenwerte und Funktionen*; Springer: Berlin, 1969; Vol. 6, Board II/5a.
- (46) (a) Srinivasan, K. R.; Kay, R. L. *J. Solution Chem.* **1977**, *6*, 357. (b) See ref 45. (c) Brazier, D. W.; Freeman, G. R. *Can. J. Chem.* **1969**, *47*, 893. (d) Gowikberg, M. G. *Chemical Equilibria and Reaction Rates at High Pressure*, 2nd ed.; Moskwa, 1960.
- (47) Miyahara, M.; Iwasaki, S.; Kotera, T.; Kawamura, T.; Okazaki, M. *J. Colloid Interface Sci.* **1995**, *170*, 335.
- (48) Williams, M. E.; Crooker, J. C.; Pyati, R.; Lyons, L. J.; Murray, R. W. *J. Am. Chem. Soc.* **1997**, *119*, 10249.
- (49) Anderson, O. S.; Feldberg, S. W. *J. Phys. Chem.* **1996**, *100*, 4622.
- (50) (a) Asano, T.; de Noble, W. J. *Chem. Rev.* **1978**, *78*, 407. (b) van Eldik, R.; Asano, T.; le Noble, W. J. *Chem. Rev.* **1989**, *89*, 549. (c) Drljaca, A.; Hubbard, C. D.; van Eldik, R.; Asano, T.; Basilevsky, M. V.; le Noble, W. J. *Chem. Rev.* **1998**, *98*, 2167.
- (51) Isaacs, N. S. *Liquid-Phase High-Pressure Chemistry*; John Wiley & Sons: Chichester, New York, Brisbane, Toronto, 1981.
- (52) (a) Nicholson, A. E.; Norrish, G. W. *Discussions Faraday Soc.* **1956**, *22*, 104. (b) Yokawa, M.; Ogo, Y. *Makromol. Chem.* **1976**, *177*, 429.
- (53) Reference 51, p 106.
- (54) Spitzer, M.; Gärtig, F.; van Eldik, R. *Rev. Sci. Instrum.* **1988**, *59*, 2092.
- (55) le Noble, W. J.; Schlott, R. *Rev. Sci. Instrum.* **1976**, *47*, 770.